Since January 2020 Elsevier has created a COVID-19 resource centre with free information in English and Mandarin on the novel coronavirus COVID-19. The COVID-19 resource centre is hosted on Elsevier Connect, the company's public news and information website.

Journal of Neuroimmunology 295–296 (2016) 60–67

Contents lists available at ScienceDirect

Journal of Neuroimmunology

journal homepage: www.elsevier.com/locate/jneuroim

T cell-derived interleukin-10 is an important regulator of the Th17 response during lethal alphavirus encephalomyelitis

Kirsten A. Kulcsar [a,b], Diane E. Griffin [a,b,*]

[a] Program in Cellular and Molecular Medicine, Johns Hopkins University School of Medicine, Baltimore, MD, 21205, USA
[b] W. Harry Feinstone Department of Molecular Microbiology and Immunology, Johns Hopkins Bloomberg School of Public Health, Baltimore, MD, 21205, USA

ARTICLE INFO

Article history:
Received 29 January 2016
Received in revised form 10 April 2016
Accepted 11 April 2016

Keywords:
Sindbis virus
Mice
Immunopathology
IL-10 source
Th17

ABSTRACT

Neuroadapted Sindbis virus infection of mice causes T cell-mediated fatal encephalomyelitis. In the absence of IL-10, pathogenic Th17 cells are increased and disease is accelerated. Lymphoid and myeloid cell contributions to IL-10 production were determined using VertX IL-10 transcriptional eGFP reporter mice. Effector and regulatory $CD4^+$ and $CD8^+$ T cells in the brain, but not the cervical lymph nodes, were the primary producers of IL-10. Th17 and Th1/Th17 cells were increased in mice that lacked T cell IL-10 production, although less than in the absence of IL-10. Morbidity and mortality were not affected suggesting an IL-10 threshold for disease exacerbation.

1. Introduction

IL-10 is an important immunoregulatory cytokine with non-redundant functions that plays a critical role in determining the balance between inflammation and immune regulation by influencing antigen presentation, T cell differentiation, cytokine production, and intensity of inflammation (Couper et al., 2008; Moore et al., 2001). A variety of cell types, including macrophages, dendritic cells, monocytes, NK cells, B cells, and T cells, can produce IL-10 (Moore et al., 2001; Saraiva and O'Garra, 2010; Wack et al., 2011) and the timing of IL-10 production after infection is key: IL-10 production prior to pathogen clearance may facilitate persistent, chronic infection, while delayed IL-10 production may foster immune-mediated pathology (Wack et al., 2011). Most investigations examining the role of IL-10 during virus infections have focused on persistent infections, but IL-10 production is also important in the pathogenesis of acute virus infections and is produced at the height of the inflammatory response during acute influenza A virus, simian virus 5, and mouse hepatitis virus (MHV) infections (Palmer et al., 2010; Puntambekar et al., 2011; Sun et al., 2009; Trandem et al., 2011b).

In mice, regulatory T cells (Tregs) producing IL-10 provide protection from lethal coronavirus infection of the CNS (Trandem et al., 2010; Zhao et al., 2014) and modulate the pathogenic Th17 response in colitis (Huber et al., 2011). These Tregs express the IL-10 receptor (IL-10R) and, in a positive feed forward loop, respond to IL-10 by producing more IL-10 (Chaudhry et al., 2011). Th17 cells also express the IL-10R and Treg-derived IL-10 restricts Th17 cell development and production of pathogenic mediators (Huber et al., 2011). The $CD8^+$ T cells that produce IL-10 are also highly cytolytic suggesting that as molecules are produced to clear infection they also begin to produce IL-10 to regulate their inflammatory capacity and modulate the consequences of the immune response (Trandem et al., 2011b). Although T cells are important producers of IL-10, intrinsic cells of the CNS can also produce IL-10 and early production at the site of infection by a virus engineered to express IL-10 provides protection against pathology later in disease (Trandem et al., 2011a). These data suggest that both early and late IL-10 production may be important in regulating the immunopathological consequences of virus infection in the CNS.

Sindbis virus (SINV) is a mosquito-borne, positive-sense RNA virus in the family *Togaviridae*. SINV, the prototypical alphavirus, is related to Venezuelan, eastern, and western equine encephalitis viruses that cause seasonal epidemics of encephalomyelitis in horses and humans (Go et al., 2014; Hollidge et al., 2010). SINV causes a mild, arthritic disease in humans, but is neuronotropic and produces encephalomyelitis in mice (Johnson, 1965; Taylor et al., 1955). Neuroadapted SINV (NSV) causes uniformly fatal disease in C57Bl/6 (B6) mice after intranasal or intracerebral infection as a result of immune-mediated damage (Greene et al., 2008; Rowell and Griffin, 2002; Thach et al., 2000) for which both $CD4^+$ and $CD8^+$ T cells have been implicated (Rowell and Griffin, 2002). IL-10 regulates this immunopathology by specifically modulating a pathogenic Th17 response that develops within the CNS

Abbreviations: 6, C57Bl/6; CLN, cervical lymph node; IL-10R, IL-10 receptor; KO, knock out; MHV, mouse hepatitis virus; NSV, neuroadapted Sindbis virus; SINV, Sindbis virus; Tregs, regulatory T cells; WT, wild type.

* Corresponding author at: W. Harry Feinstone Department of Molecular Microbiology and Immunology, Johns Hopkins Bloomberg School of Public Health, 615 N. Wolfe St, E5636, Baltimore, MD 21205, United States.
E-mail address: dgriffi6@jhu.edu (D.E. Griffin).

http://dx.doi.org/10.1016/j.jneuroim.2016.04.010
0165-5728/

of susceptible B6 mice in response to infection (Kulcsar et al., 2014). Tregs are implicated as a source of IL-10 because in resistant Balb/cJ mice a robust IL-10-producing Treg response is associated with survival (Kulcsar et al., 2015). Therefore, IL-10 is an important immune modulator during NSV infection, but the cellular sources of this cytokine in the CNS and their relative importance during lethal infection are not known.

To determine what cell types produce IL-10 during NSV infection, we utilized VertX IL-10 mRNA reporter mice (Madan et al., 2009) to identify IL-10-expressing cells without the need for *ex vivo* stimulation. Analysis of these mice showed that IL-10 was expressed in the CNS after infection, but not in the draining cervical lymph nodes, and that the predominant IL-10-expressing cells were $CD4^+$ and $CD8^+$ T cells, with little contribution from myeloid cells. Within the $CD4^+$ T cell compartment $CD25^+$ and $CD25^-$ cells expressed IL-10. Examination of mice deficient in IL-10 production specifically in T cells (IL-10^{CD4KO}) or in myeloid cells (IL-10^{LysMKO}) identified T cells as the predominant source of IL-10 that restricts Th17 as well as Th1/Th17 cell development in the CNS. These data show that T cell-derived IL-10 is critical for regulation of the immune response during an acute lethal CNS alphavirus infection.

2. Materials and methods

2.1. Mice and infection

C57Bl/6J (B6), B6.129P2-Il10^{tm1Cgn}/J (C57Bl/6 IL-$10^{-/-}$) (Kuhn et al., 1993), and B6.129P2-*Lyzs*$^{tm1(cre)Ifo}$/J (C57Bl/6 LysM^{Cre}) (Clausen et al., 1999) mice were purchased from Jackson Laboratories (Bar Harbor, ME). IL-10eGFP reporter (VertX) mice on a B6 background, were kindly provided by Dr. Christopher Karp (Cincinnati Children's Hospital) (Madan et al., 2009). *Il10*$^{flox/flox}$ × *CD4*^{Cre} (IL-$10^{CD4\text{-}KO}$) mice on a B6 background were kindly provided by Dr. Werner Muller (University of Manchester) (Roers et al., 2004). *Il10*$^{flox/flox}$ × *LysM*^{Cre} (IL-$10^{LysM\text{-}KO}$) mice were generated in house (Siewe et al., 2006). Mice were sex-matched and intranasally infected at 4–6 weeks of age with 10^5 PFU NSV (Jackson et al., 1988) diluted in 20 μL HBSS. For assessment of morbidity and mortality, mice were monitored daily using the following scoring system: 0) no clinical signs, 1) abnormal hind-limb and tail posture, ruffled fur, and/or hunched back, 2) unilateral hind-limb paralysis, 3) bilateral hind-limb paralysis or full-body paralysis, and 4) dead. For tissue collection, mice were anesthetized with isoflurane and bled *via* cardiac puncture. Mice were perfused with ice-cold PBS and brains and spinal cords were collected and used fresh or snap frozen and stored at −80 °C. All experiments were performed according to protocols approved by the Johns Hopkins University Institutional Animal Care and Use Committee.

2.2. Gene expression analysis using quantitative real-time RT-PCR

RNA was isolated from frozen tissue using the RNeasy Lipid Mini RNA Isolation Kit (Qiagen). RNA was quantified using a nanodrop spectrophotometer and cDNA was prepared with the High Capacity cDNA Reverse Transcription Kit (Life Technologies) using 2.5 μg of input RNA. Quantitative real-time PCR was performed using 2.5 μL cDNA, the PrimeTime Mouse IL-10 assay (Integrated DNA Technologies), and 2× Universal PCR Mastermix (Applied Biosystems). *Gapdh* mRNA levels were determined using the rodent primer and probe set (Applied Biosystems). All reactions were run on an Applied Biosystems 7500 Real-time PCR machine with the following conditions: 50 °C for 2 min, 95 °C for 10 min, 95 °C for 15 s, and 60 °C for 1 min for 50 cycles. Transcript levels were determined by normalizing the target gene Ct value to the Ct value of the endogenous housekeeping gene *gapdh*. This normalized value was used to calculate the fold-change relative to the average of the uninfected control (ΔΔCt method).

2.3. Mononuclear cell isolation

Single-cell suspensions from brain and spinal cord tissues were prepared as previously described (Kulcsar et al., 2014). Briefly, tissues were homogenized using the GentleMACS system (Miltenyi) with enzymatic digestion (RPMI + 1% FBS, 1 mg/mL collagenase and 0.1 mg/mL DNase [Roche]). The homogenate was filtered through a 70 μm filter and myelin debris and red blood cells were removed by centrifuging the single-cell suspension on a 30/70% discontinuous percoll gradient for 30 min at 4 °C. Mononuclear cells at the interface were collected, resuspended in PBS + 2 mM EDTA, and live cells were identified using trypan blue exclusion and counted.

2.4. Flow cytometry

Approximately 1–2 × 10^6 cells were used for immunophenotyping by flow cytometry. Cells were stained with the violet Live/Dead Fixable Cell Stain kit (Invitrogen) in PBS + 2 mM EDTA, blocked using rat anti-mouse CD16/CD32 (BD Pharmingen), diluted in PBS + 2 mM EDTA + 0.5% BSA, surface stained for 25 min on ice, fixed, and resuspended in 200 μL of PBS + 2 mM EDTA + 0.5% BSA. All antibodies were from BD Pharmingen or eBioscience: CD45 (clone 30-F11), CD11b (clone M1-70), Ly6G (clone 1A8), Ly6C (clone HK1.4), CD3 (clone 17A2), CD4 (clone RM4-5), CD8 (clone 53-6.7), and CD25 (clone CP61.5). Cell types were defined as follows: microglia ($CD45^{lo}CD11b^+Ly6G^-Ly6C^-$), macrophages/monocytes ($CD45^{hi}CD11b^+Ly6G^-Ly6C^+$), neutrophils ($CD45^+CD11b^+Ly6G^+Ly6C^{int}$), T cells ($CD3^+$), CD4 T cells ($CD3^+CD4^+$), and CD8 T cells ($CD3^+CD8^+$).

For determination of T cell cytokine production and foxp3 expression, 2–3 × 10^6 cells in RPMI + 1% FBS were stimulated with 50 ng/mL PMA and 1 μg/mL ionomycin in the presence of GolgiPlug-brefeldin A (BD Pharmingen) for 4 h. Cells were washed and live/dead staining, blocking, and surface staining were performed as described above. After surface staining, cells were fixed and permeabilized using either the CytoFix/CytoPerm kit (BD Pharmingen) and stained for intracellular proteins 25 min on ice, and resuspended in 200 μL of PBS + 2 mM EDTA + 0.5% BSA. Antibodies used were: IFNγ (clone XMG1.2) and IL-17a (clone eBio17B7). Data were acquired using a BD FACS Canto II with FACS Diva software (version 6.0), and analyzed using FlowJo 8.8.7 (TreeStar Inc.).

2.5. Statistical analysis

Data from 2 to 4 independent experiments or at least 3 mice per group were used for analysis. Survival was compared using Kaplan–Meier survival curves (log rank test). Multiple groups were compared over time using a one-way ANOVA with a Dunn post-test at each time point. Two groups over time were compared using a two-way ANOVA with a Bonferroni post-test or at a single time point using an unpaired, two-tailed Student's t test with a 95% confidence interval. All statistical analyses were done using Graph Prism 5 (GraphPad).

3. Results

3.1. Expression of IL-10eGFP in NSV-infected mice occurs primarily in the brain, not the draining cervical lymph nodes

IL-10 is an important immunoregulatory molecule during a variety of infections (Couper et al., 2008; Wack et al., 2011). During virus infections of the CNS IL-10 plays an important role in limiting inflammation and protecting against death during acute infections and protecting against demyelination during chronic infections (Lin et al., 1998; Trandem et al., 2011a; Zhao et al., 2014). Previously, we showed that IL-10 was an important cytokine for immune modulation and protection during NSV infection (Kulcsar et al., 2015; Kulcsar et al., 2014). To determine the cell type(s) responsible for IL-10 production, we utilized

VertX IL-10 mRNA reporter mice (Madan et al., 2009). VertX mice express eGFP under control of an internal ribosomal entry site placed immediately downstream of the stop codon and before the poly-A site for IL-10 and do not affect IL-10 protein production (Madan et al., 2009).

The cervical lymph nodes (CLNs) and brains of VertX mice infected intranasally with 1×10^5 pfu NSV were evaluated for cells expressing IL-10eGFP. There were few IL-10eGFP$^+$ cells in the CLNs at any time after infection. Three days after infection, 0.44% of cells were IL-10eGFP$^+$ and this increased to only 1.41% at 5 d and 1.58% at 7 d after infection (Fig. 1A, B). In the brain, the number and frequency of IL-10eGFP$^+$ cells increased substantially during the course of infection. Few IL-10eGFP$^+$ cells were present 3 d after infection (0.1%, 430 cells/brain). However, by 5 d the number of IL-10eGFP$^+$ cells began to increase (0.61%, 8×10^3 cells) and the increase continued through 7 d with 8.5% of cells and approximately 4×10^5 IL-10eGFP$^+$ cells in the brain of each animal (Fig. 1A, C). Therefore, IL-10-producing cells were found infrequently in the CLNs, but often in the brains of NSV-infected mice and were most abundant 7 d after infection, a time of peak inflammation.

3.2. T cells are the primary cells expressing IL-10eGFP in the brains of NSV-infected mice

To determine the cell type-specific expression of IL-10 during NSV infection, we used flow cytometry to assess IL-10eGFP expression in monocytes/macrophages, microglia, neutrophils, and CD3$^+$ T cells 5 and 7 d after infection. Evaluation of myeloid cells was difficult due to autofluorescence. To compensate for this, we subtracted the FITC

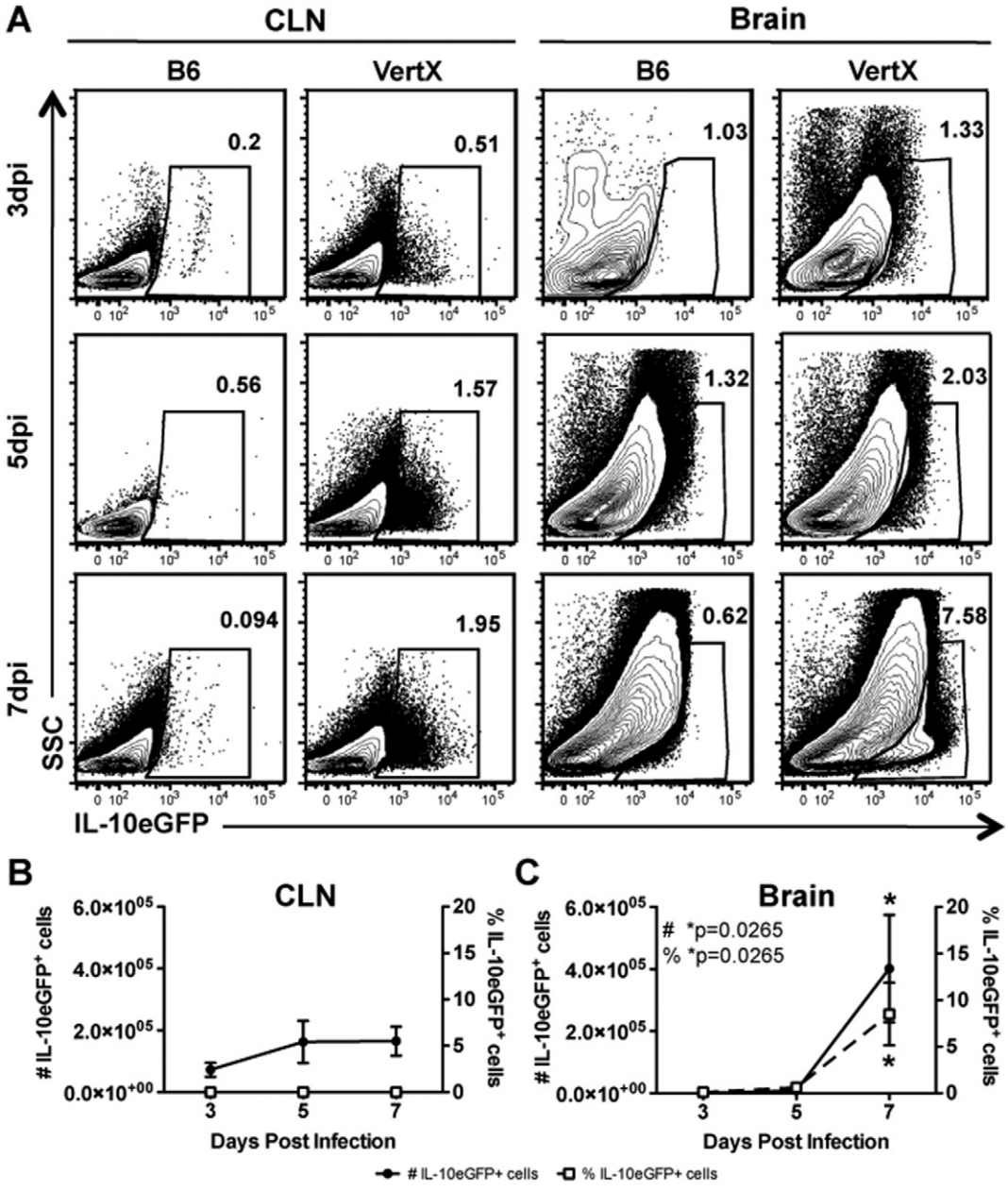

Fig. 1. IL-10eGFP$^+$ cells increased in the brain, but not the cervical lymph nodes, during NSV infection. VertX and WT mice were infected intranasally with 10^5 pfu of NSV and assessed at 3, 5, and 7 d after infection. (A) Flow cytometric analysis of IL-10eGFP expression in cells isolated and pooled from the cervical lymph nodes (n = 4–6) and brains (n = 4–12) of VertX mice. The IL-10eGFP$^+$ gate was set using cells from WT mice as the negative control at each time point. The contour plots are representative of 3 independent experiments. (B–C) The absolute number of IL-10eGFP$^+$ cells per animal (closed circle, solid line) and frequency of IL-10eGFP$^+$ cells (% of live cells) (open squares, dashed line) were determined at each time point in the cervical lymph nodes (B) and brains (C) of mice by subtracting the background signal observed in B6 mice in each tissue at each time point. The data represent the mean ± SEM from 3 independent experiments. *P < 0.05.

channel signal from WT mice for all cell types at the same time points to determine the level of eGFP expression above background. Five days after infection, 7.14% of T cells expressed IL-10eGFP, which was higher than the percentage of microglia expressing IL-10eGFP (0.66%, P = 0.0051) (Fig. 2A, B). Although the percentage of IL-10eGFP$^+$ T cells was greater than that of neutrophils (1.96%) and monocyte/macrophages (2.87%), the differences were not significant (Fig. 2A, B). By 7 d after infection, the frequency of IL-10eGFP$^+$ T cells increased to 55.1% and was significantly greater than the percentage of IL-10eGFP$^+$ microglia (2.0%, P = 0.0007), monocyte/macrophages (13.5%, P = 0.0447) or neutrophils (5.29%, P = 0.0024) (Fig. 2A, C). These data suggest that T cells serve as the primary source of IL-10 during NSV infection.

We next evaluated the relative contributions of myeloid cells and T cells to overall IL-10 production in the brain using mice selectively deficient for IL-10 production in either T cells or myeloid cells. IL-10 flox/flox mice (IL-10$^{fl/fl}$) were crossed to CD4-Cre and to LysM-Cre mice to produce mice that were deficient in IL-10 production from CD4$^+$ and CD8$^+$ T cells (IL-10$^{CD4\text{-}KO}$) or myeloid cells (IL-10$^{LysM\text{-}KO}$) (Roers et al., 2004; Siewe et al., 2006). IL-10 gene expression in the brains of WT, IL-10$^{CD4\text{-}KO}$, and IL-10$^{LysM\text{-}KO}$ mice was then evaluated during NSV infection. Levels of *Il10* mRNA were similar in the brains of WT mice and IL-10$^{LysM\text{-}KO}$ mice throughout infection (Fig. 3). In contrast, *Il10* mRNA levels in the brains of IL-10$^{CD4\ KO}$ mice were significantly lower during the course of infection (P = 0.0009), particularly at 7 d (P < 0.001) (Fig. 3). Together these data suggest that T cells are the primary producers of IL-10 in the brain during NSV infection and in the absence of T cell-derived IL-10 there was very little *Il10* mRNA expressed.

3.3. Both CD4$^+$ and CD8$^+$ T cells contribute to IL-10 production in the CNS during NSV infection

CD4$^+$ and CD8$^+$ T cells can produce IL-10 in the context of virus infection and lead to dampening of the immune response as well as virus persistence (Couper et al., 2008). Previous studies have shown that individual T cell subsets produce IL-10 with different kinetics during acute and persistent CNS viral infections (Puntambekar et al., 2011; Trandem et al., 2011b; Zhao et al., 2014). IL-10 production selectively knocked-out in CD4$^+$ and CD8$^+$ T cells significantly reduced the amount of *Il10* mRNA expressed (Fig. 3). To determine the dynamics of IL-10 production by CD4$^+$ and CD8$^+$ T cells, T cell subsets were evaluated in VertX mice for expression of IL-10eGFP in the brain 5 d and 7 d after infection and in the spinal cord at 7 d when there were enough T cells to reliably detect IL-10eGFP expression (Fig. 4). Both CD4$^+$ and CD8$^+$ T cells in the brains and spinal cords of NSV-infected mice expressed IL-10eGFP. The numbers of CD4$^+$ IL-10eGFP$^+$ cells increased from 1.87×10^3 cells per brain 5 d after infection to 3.63×10^4 cells per brain 7 d after infection (P = 0.0382, Fig. 4A, C). The numbers of

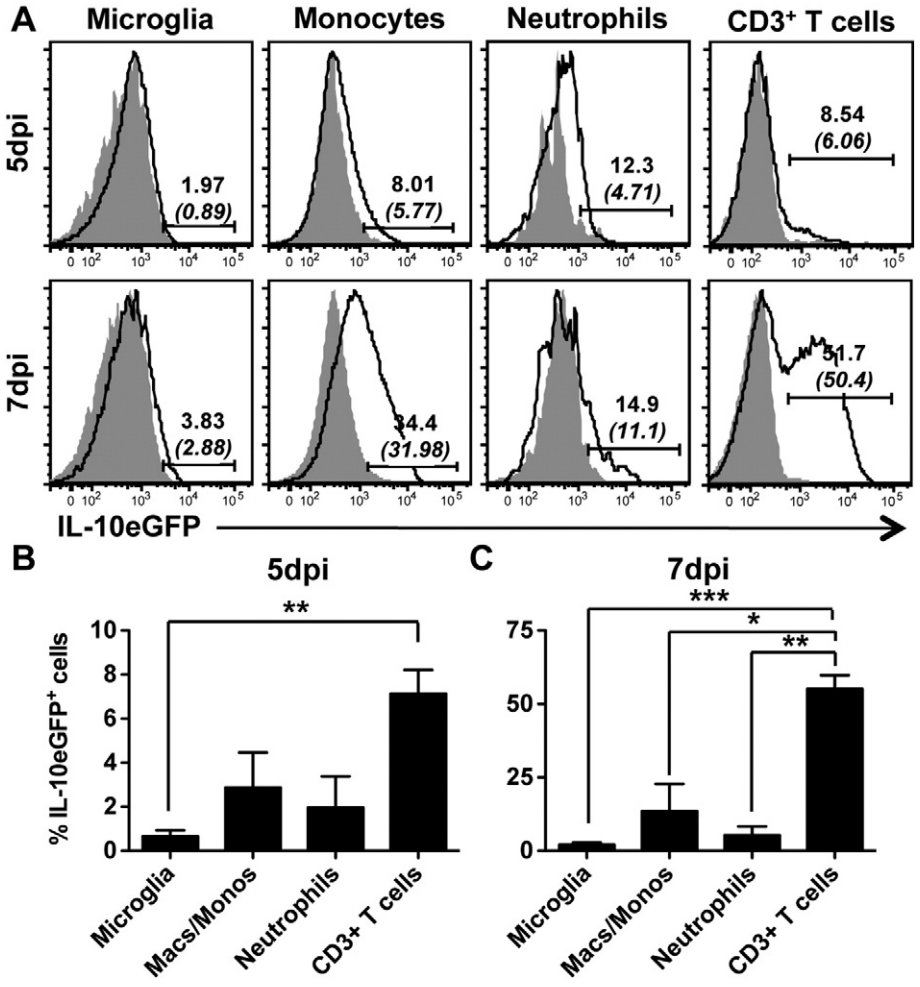

Fig. 2. IL-10eGFP expression is most prevalent in CD3$^+$ T cells in the brains of NSV-infected mice 5 and 7 d after infection. VertX and WT mice were infected intranasally with 10^5 pfu of NSV and assessed 5 and 7 d after infection for cell type-specific expression of IL-10eGFP. (A) Microglia, monocytes, neutrophils, and CD3$^+$ T cells isolated from the brains of VertX mice (pooled, n = 4–12) were assessed for IL-10eGFP expression using flow cytometry. The IL-10eGFP$^+$ populations (black line) are shown relative to WT cells (gray, filled) for each cell population. The histograms are representative of 2–3 independent experiments. The values in parentheses are percent of positive cells after removing background. (B, C) The frequency of IL-10eGFP$^+$ cells (% of live cells) was determined at 5 (B) and 7 (C) d after infection by subtracting the background signal observed in WT mice in each cell type at each time point. The data represent the mean ± SEM from 2 to 3 independent experiments. *P < 0.05, **P < 0.01, ***P < 0.001.

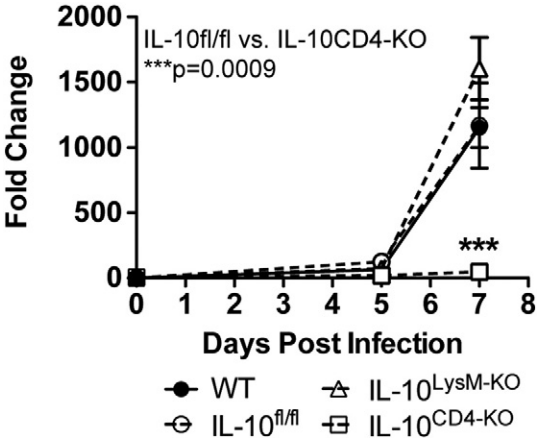

Fig. 3. T cells are the primary source of *Il10* mRNA in the brain during NSV infection. WT, IL-$10^{fl/fl}$, IL-$10^{CD4\text{-}KO}$, and IL-$10^{LysM\text{-}KO}$ mice were infected intranasally with 10^5 pfu of NSV and brain tissue was collected from mice before infection and 5 and 7 d after infection. *Il10* mRNA expression was measured by qRT-PCR. Ct values were normalized to GAPDH and fold change was calculated relative to uninfected controls (ΔΔCt). Data were pooled from 2 independent experiments and represent the mean ± SEM of 3–6 mice at each time point. ***$P < 0.001$.

$CD8^+$ IL-10eGFP$^+$ cells also increased from 1.74×10^3 cells per brain 5 d after infection to 1.56×10^5 cells per brain 7 d after infection ($P = 0.0281$, Fig. 4A, C). The frequency of $CD4^+$ and $CD8^+$ T cells expressing IL-10eGFP also significantly increased from 5 d to 7 d after infection (CD4: 5 d 10.2% *vs.* 7 d 33.8%, $P = 0.0369$; CD8: 5 d 8.8% *vs.* 7 d 57.1%, $P = 0.0470$) (Fig. 4A, B). Not only were more $CD4^+$ and $CD8^+$ T cells present 7 d after infection, but more cells within each population were expressing IL-10 than at 5 d.

We also compared IL-10eGFP expression between $CD4^+$ and $CD8^+$ T cells. Five days after infection there were similar numbers as well as similar percentages of $CD4^+$ and $CD8^+$ T cells that expressed IL-10eGFP (Fig. 4A–C). By 7 d after infection, however, there was a higher frequency as well as a greater number of $CD8^+$ T cells that expressed IL-10eGFP compared to $CD4^+$ T cells, although this did not reach statistical significance (Fig. 4A–C). A similar trend was present in the spinal cord 7 d after infection where more $CD8^+$ T cells expressed IL-10eGFP$^+$ compared to $CD4^+$ T cells (Fig. 4A–C).

These data suggest that during the initial stages of T cell infiltration into the CNS, both $CD4^+$ and $CD8^+$ T cells contribute similarly to IL-10 production; however, as inflammation increases, $CD8^+$ T cells become the dominant source of IL-10. Furthermore, both $CD4^+$ and $CD8^+$ T cells also contribute to IL-10 production in the spinal cord.

3.4. Tregs and IL-10 expression

To determine if Tregs contribute to IL-10 production, we characterized these cells and their IL-10 expression 5 d and 7 d after infection (Fig. 5). Our previous studies showed that both $CD4^+CD25^+foxp3^-$ and $CD4^+CD25^+foxp3^+$ cells express IL-10 during NSV infection in both B6 and Balb/c mice (Kulcsar et al., 2015). In VertX mice, both $CD4^+CD25^-$ and $CD4^+CD25^+$ T cells expressed IL-10eGFP. The number of $CD4^+CD25^-$ cells increased from 1.37×10^3 cells 5 d after infection to 2.5×10^4 cells 7 d after infection ($P = 0.0433$, Fig. 5A, C). Similarly, the number of $CD4^+CD25^+$ cells increased from 637 cells 5 d after infection to 1.24×10^4 cells 7 d after infection ($P = 0.0157$, Fig. 5A, C). The percentage of $CD4^+CD25^-$ cells that expressed IL-10eGFP increased from 8.4% at 5 d to 26.0% at 7 d after infection ($P = 0.0145$) while the percentage of $CD4^+CD25^+$ cells expressing IL-10eGFP increased from 19.2% at 5 d to 36.0% 7 d after infection (Fig. 5A, B). Within the $CD4^+CD25^+$ population there was a higher frequency of IL-10eGFP$^+$ cells than in the $CD4^+CD25^-$ population 5 and 7 d after infection, although this did not reach statistical significance (Fig. 5B). There were, however,

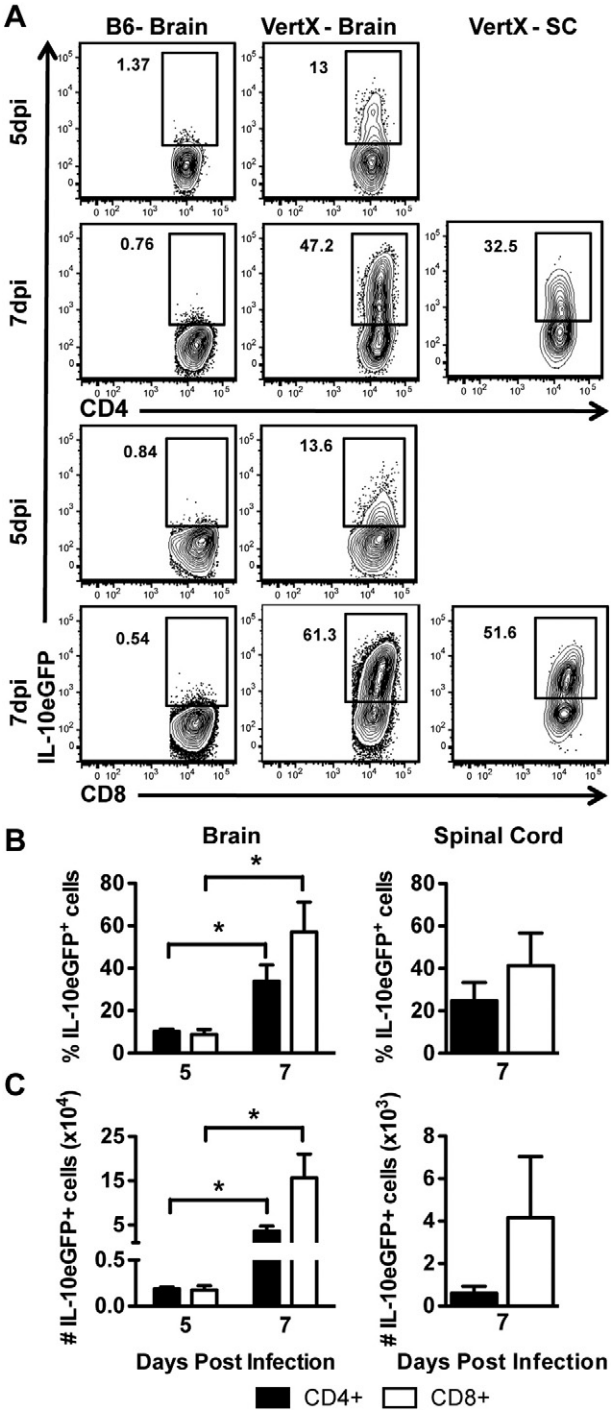

Fig. 4. $CD4^+$ and $CD8^+$ T cells express IL-10eGFP in the brains and spinal cords of mice during NSV infection. VertX and WT mice were infected intranasally with 10^5 pfu of NSV and $CD4^+$ and $CD8^+$ T cells in the CNS were assessed for IL-10eGFP expression 5 and 7 d after infection *via* flow cytometry. (A) Flow cytometric analysis of IL-10eGFP expression in cells isolated and pooled from the brains (n = 4–12) and spinal cords (SC) (n = 4–12) of VertX mice. The IL-10eGFP$^+$ gate was set using cells from B6 mice as the negative control at each time point. The contour plots are representative of 3 independent experiments. The frequency (% of live cells) (B) and absolute number per animal (C) of IL-10eGFP$^+$ cells 5 and 7 d after infection in the brains of VertX mice and 7 d after infection in the spinal cords. Data represent the mean ± SEM from 3 independent experiments. *$P < 0.05$.

significantly more $CD4^+CD25^-$IL10eGFP$^+$ cells than $CD4^+CD25^+$-IL10eGFP$^+$ cells 5 d after infection ($P = 0.0064$), a trend that was maintained at 7 d (Fig. 5C). These data show that within the $CD4^+$ T cell compartment, there were more $CD25^-$ than $CD25^+$ cells expressing

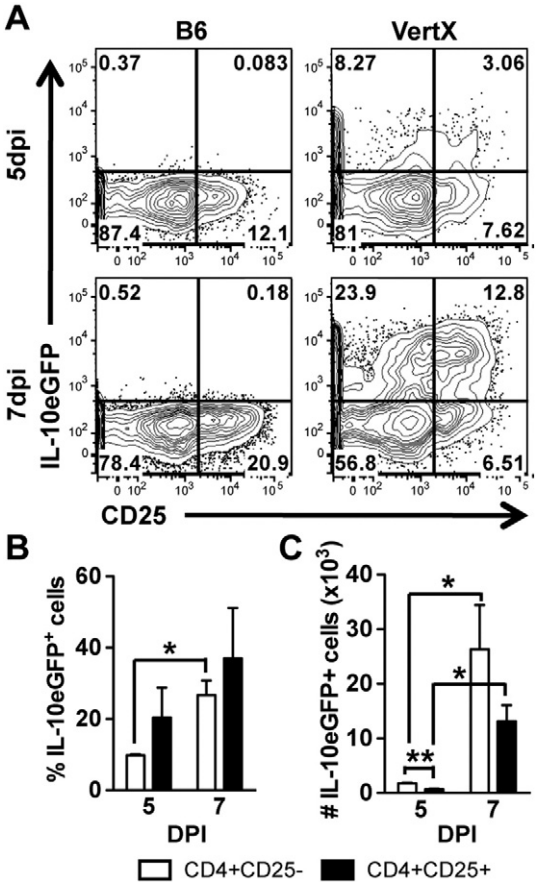

Fig. 5. Regulatory T cells produce IL-10 in the brains of NSV-infected mice. (A–C) WT and VertX mice were infected intranasally with 10^5 pfu of NSV and cells were isolated and pooled (n = 4–12) from brains 5 and 7 d after infection. Cells were stained for the presence of CD3, CD4, and CD25 and IL-10eGFP expression was evaluated using flow cytometry. (A) Contour plots are representative of 3 independent experiments. (B) The frequency of IL-10eGFP$^+$ cells (% of CD4$^+$CD25$^-$ (white bar) and % of CD4$^+$CD25$^+$ (black bar)) and (C) absolute number of CD4$^+$CD25$^-$IL-10eGFP$^+$ (white bar) and CD4$^+$CD25$^+$IL-10eGFP$^+$ (black bar) cells was calculated for each time point. The data are pooled from three independent experiments and are presented as the mean ± SEM. *P < 0.05, **P < 0.01.

IL-10 during NSV infection, but a similar proportion within each population were IL-10eGFP$^+$.

3.5. T cell-derived IL-10 contributes to the regulation of the pathogenic Th17 response

A primary role for IL-10 during NSV infection is regulation of the pathogenic Th17 response. In the absence of IL-10, more pathogenic Th17 cells, as well as Th1/Th17 cells, are present in the CNS at the onset of paralysis and contribute to accelerated morbidity and mortality (Kulcsar et al., 2014). In WT mice, the primary source of IL-10 is T cells, not myeloid cells (Fig. 3). To verify that IL-10 produced by T cells is responsible for regulating the Th17 response during viral encephalomyelitis, we compared the CD4$^+$ T cell skewing of IL-10$^{CD4\text{-}KO}$ and IL-10$^{LysM\text{-}KO}$ mice to IL-10$^{fl/fl}$ littermates, WT, and IL-10 KO mice. Cells isolated from brains 5 d after infection, when differences in the Th17 response between WT and IL-10 KO mice are the greatest (Kulcsar et al., 2014), were stimulated *ex vivo*. To identify Th1, Th17, and Th1/Th17 responses, CD4$^+$ T cells were evaluated for the production of IFNγ, IL-17a, and co-production of IFNγ and IL-17a, respectively (Fig. 6). There were no significant differences in the Th1 responses as measured by numbers or percentages of IFNγ-producing CD4$^+$ T cells. However, the Th17 responses were different (Fig. 6A–C). As expected, WT and IL-10$^{fl/fl}$ mice had similar Th17 responses while in IL-10 KO mice there was a higher percentage (P = 0.0011; Fig. 6A, F) and more (P = 0.0422; Fig. 6G) CD4$^+$ IL-17a$^+$ T cells than in WT mice. IL-10$^{CD4\text{-}KO}$ mice also had an increased Th17 response compared to IL-10$^{fl/fl}$ littermates. Approximately 2.3% of the CD4$^+$ T cells from IL-10$^{fl/fl}$ mice produced IL-17a compared to 5.3% in IL-10$^{CD4\text{-}KO}$ mice (P = 0.0072; Fig. 6A, F). This resulted in almost twice as many CD4$^+$IL-17a$^+$ T cells in the IL-10$^{CD4\text{-}KO}$ mice (P = 0.0018; Fig. 6G). The IL-10$^{LysM\text{-}KO}$ mice had Th17 responses similar to WT and IL-10$^{fl/fl}$ mice (Fig. 6F, G).

As previously observed (Kulcsar et al., 2014), IL-10 KO mice had a significantly higher frequency of IL-17a$^+$IFNγ$^+$ cells within the CD4$^+$ T cell compartment compared to WT mice (P = 0.0421, Fig. 6D) resulting in more CD4$^+$IL-17a$^+$IFNγ$^+$ cells in the brains of IL-10 KO mice than WT mice (Fig. 6G). Interestingly, IL-10$^{CD4\text{-}KO}$ mice also had a significantly higher frequency of IL-17a$^+$IFNγ$^+$ double-producing CD4 + T cells compared to IL-10$^{fl/fl}$ mice (P = 0.0298, Fig. 6D), as well as more of these cells (P = 0.0461, Fig. 6G). Together these data confirm the importance of IL-10 as a regulator of both the Th17 and Th1/Th17 responses. Furthermore, the data show that in the absence of T cell-derived IL-10, but not myeloid cell-derived IL-10, this response is exacerbated.

To determine whether mice lacking T cell-derived IL-10 also had accelerated morbidity and mortality as observed in IL-10 KO mice IL-10$^{fl/fl}$, IL-10$^{CD4\text{-}KO}$, and IL-10$^{LysM\text{-}KO}$ mice infected with NSV were monitored daily for clinical disease. The IL-10$^{LysM\text{-}KO}$ mice showed no difference in the course of disease or the time of death compared to IL-10$^{fl/fl}$ mice consistent with their similar Th1 and Th17 responses (Fig. 7C, D). However, IL-10$^{CD4\text{-}KO}$ also had a similar course of disease compared to IL-10$^{fl/fl}$ mice (Fig. 7A, B). Although the Th17 response was elevated in IL-10$^{CD4\text{-}KO}$ mice, it was less than observed in IL-10 KO mice suggesting that a threshold for an increase in disease severity was not reached. Together these data show that T cell-derived IL-10 is important in dampening pathogenic Th17 responses, but either that other mechanisms also contribute or that small amounts of locally produced IL-10 by myeloid cells are sufficient to modulate disease.

4. Discussion

IL-10 restricts the pathogenic Th17 response in the CNS and is an important determinant of survival from alphavirus encephalomyelitis (Kulcsar et al., 2015; Kulcsar et al., 2014). These studies of VertX IL-10-reporter mice infected with NSV showed that IL-10-producing cells were increasingly abundant in the brain and spinal cord after infection, but infrequent in the draining CLN. The numbers of IL-10eGFP$^+$ cells in the CNS were primarily CD4$^+$ and CD8$^+$ T cells and within the CD4$^+$ T cell population, more IL-10eGFP$^+$ cells were CD25$^-$ than CD25$^+$ at the height of inflammation. In the absence of T cell-derived IL-10 in IL-10$^{CD4\ KO}$ mice, numbers of Th17 and Th1/Th17 cells increased, although not as much as in IL-10 KO mice, and the course of disease was not altered. Therefore, effector, as well as regulatory CD4$^+$ and CD8$^+$ T cells differentiated in the CNS to become important sources of IL-10 that modulated the inflammatory response and development of Th17 and Th1/Th17 cells.

Cells in the brain and spinal cord produced IL-10, whereas few IL-10-expressing cells were found in the draining CLN indicating acquisition of this function after entry into the CNS. Tissue-specific expression of IL-10 also occurs during CNS infection with the gliatropic JHM strain of MHV (Puntambekar et al., 2011; Trandem et al., 2011b). These data suggest that although virus-specific T cells are generated in the draining CLN, they do not begin producing IL-10 until they reach the site of infection. Similarly, during influenza virus infection the majority of IL-10$^+$ T cells are in the lung, not in the draining LN or spleen (McKinstry et al., 2009). However, a recent study showed that with *ex vivo* stimulation virus-specific Tregs in the draining CLNs do produce IL-10 (Zhao et al., 2014) suggesting that some T cell subsets are programmed to produce this regulatory cytokine prior to encountering the milieu of the inflamed CNS. Together, these data suggest that T cell production of IL-10 is

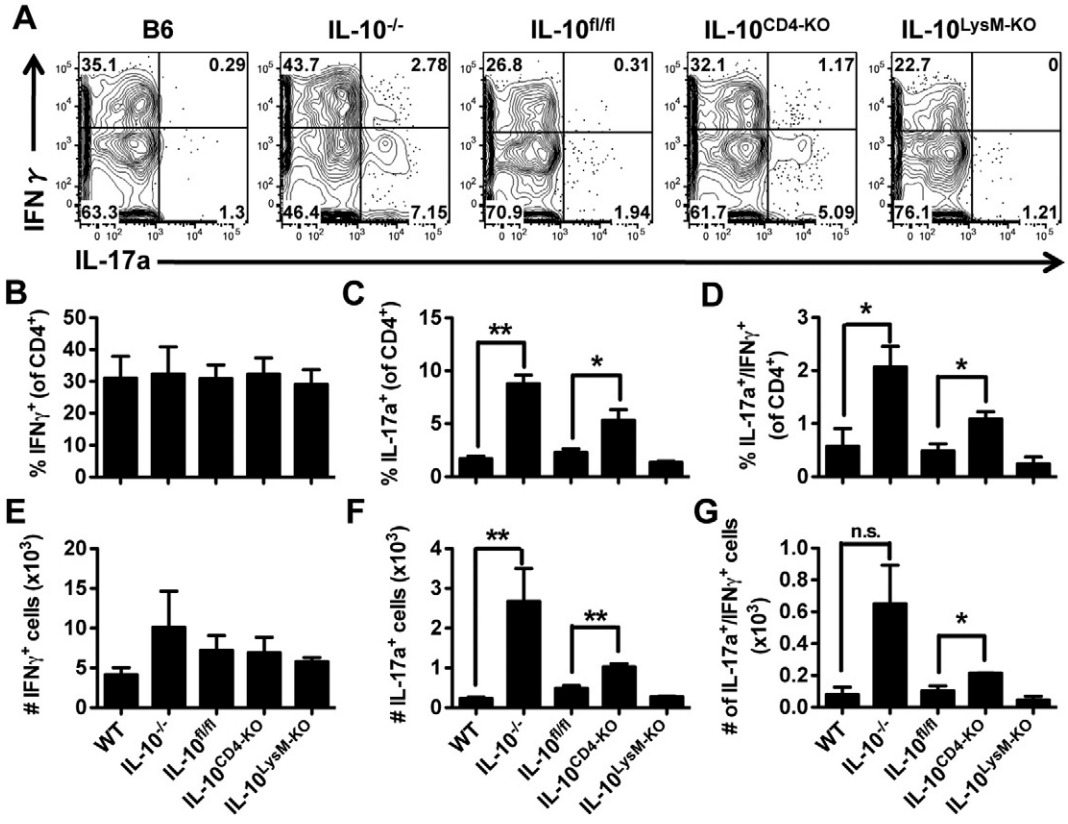

Fig. 6. IL-10 produced by T cells, but not myeloid cells, contributes to controlling the Th17 and Th1/Th17 response in the brain during NSV infection. WT, IL-10KO, IL-$10^{fl/fl}$, IL-$10^{CD4\text{-}KO}$, and IL-$10^{LysM\text{-}KO}$ mice were infected intranasally with 10^5 pfu of NSV. Cells were isolated from the brain 5 days after infection and pooled (n = 2–4). The mononuclear cells were stimulated *ex vivo* with PMA and ionomycin and subsequently stained for the surface markers CD3 and CD4 followed by intracellular cytokine staining for IFNγ and IL-17a to identify Th1 and Th17 cells, respectively. (A) Contour plots showing $CD4^+$ $IFN\gamma^+$ and $CD4^+$ $IL\text{-}17a^+$ cells are representative of 3–6 independent experiments. The percentages of $CD4^+$ T cells that produced IFNγ (B), IL-17a (C) and IFNγ and IL-17a (D) were determined for all groups. The absolute numbers of $CD4^+$ $IFN\gamma^+$ (E), $CD4^+$ $IL\text{-}17a^+$ (F) and $CD4^+$ $IFN\gamma^+$ $IL\text{-}17a^+$ (G) T cells were determined for all groups. The data are pooled from 3 to 6 independent experiments and are presented as the mean ± SEM. *P < 0.05, **P < 0.01, ***P < 0.001.

dependent on the environment and the level of stimulation (Saraiva and O'Garra, 2010). Contributing factors may include the local presence of cytokines that stimulate IL-10 production such as IL-6 and TGF-β (Li and Flavell, 2008, Lee et al., 2013).

Once in the CNS, T cells were the primary producers of IL-10 during NSV infection (Puntambekar et al., 2011; Trandem et al., 2011b) with similar contributions from $CD4^+$ and $CD8^+$ T cells initially. However, by 7 d after infection the proportion of $CD8^+$ T cells that expressed IL-10eGFP$^+$ was higher than that of $CD4^+$ T cells so that at the peak of inflammation $CD8^+$ T cells were the primary producers of IL-10. This may correlate with an increase in $CD8^+$ T cell cytolytic activity as seen during MHV infection (Trandem et al., 2011b).

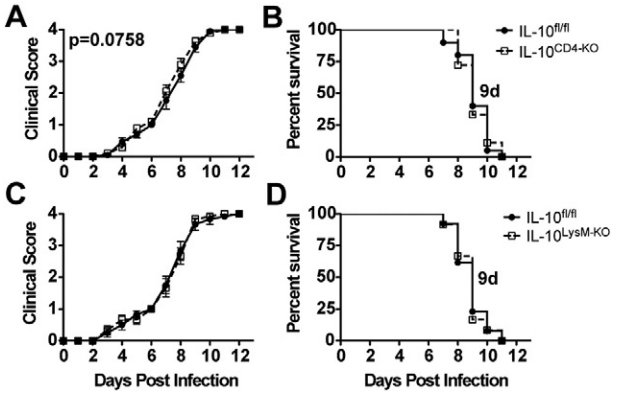

Fig. 7. Lack of T cell or myeloid IL-10 production does not affect the disease outcome. IL-$10^{fl/fl}$, IL-$10^{CD4\text{-}KO}$, and IL-$10^{LysM\text{-}KO}$ mice were infected intranasally with 10^5 pfu of NSV and monitored daily for clinical signs. (A, C) Clinical score scale: 0, no signs; 1, abnormal hind limb and tail posture, ruffled fur, hunched back; 2, unilateral hind-limb paralysis; 3, bilateral hind limb paralysis and/or moribund; and 4, dead. Data were pooled from 3 independent experiments and are presented as the mean ± SEM. (B, D) Survival was assessed using a Kaplan–Meier analysis and log-rank test. Survival was 0% with a mean day of death of 9 d after infection for all groups. Data were pooled from 3 independent experiments. IL-$10^{fl/fl}$ and IL-$10^{CD4\text{-}KO}$ n = 19–20, IL-$10^{fl/fl}$ and IL-$10^{LysM\text{-}KO}$ n = 12.

IL-10 production and a robust regulatory T cell response are both associated with protection from lethal disease induced by NSV infection (Kulcsar et al., 2015). In the brain 7 d after NSV infection there were more IL-10eGFP$^+$ $CD4^+$ cells in the $CD25^-$ compartment than the $CD25^+$ compartment indicating that effector, as well as regulatory, $CD4^+$ T cells contributed to IL-10 production in the CNS during NSV infection. However, during MHV infection of the CNS more $CD25^+$ than $CD25^-$ cells were IL-10eGFP$^+$ 7 d after infection (Puntambekar et al., 2011). The numbers of both $CD4^+CD25^+$ $foxp3^+$ and $foxp3^-$ T cells producing IL-10 increased as inflammation increased and both can inhibit pathogenic Th17 responses (Huber et al., 2011). Therefore, multiple $CD4^+$ T cell subsets contribute to IL-10 production in the CNS during NSV infection.

Complete absence of IL-10 increases the pathogenic Th17 and Th1/Th17 response to NSV infection and results in more rapid disease onset and death (Kulcsar et al., 2014). A significant increase in the Th17 and Th1/Th17 response in mice lacking T cell-derived IL-10, but not in mice lacking myeloid cell-derived IL-10, indicated that T cells were the primary source of IL-10 regulating the CNS development of Th17 cells. However, the increase of Th17 cells in IL-$10^{CD4\ KO}$ mice was less than that observed in mice completely deficient in IL-10 and did not have a significant impact on the course of disease. These data suggest that although T cell-derived IL-10 modulates the Th17 and Th1/Th17 responses, other sources of IL-10 also participate in regulation.

Most microglia and dendritic cells from lymphoid tissues do not express LysM, thus these cells will maintain the ability to produce IL-10 in the IL-$10^{LysM\ KO}$ mice (Clausen et al., 1999; Goldmann et al., 2013; Siewe et al., 2006) even if it is at low levels. These cells may modulate the Th17 response by locally producing IL-10 and affecting T cell differentiation.

In summary, $CD4^+$ and $CD8^+$ T cells were the primary producers of IL-10 in the CNS during NSV infection. Within the $CD4^+$ T cell population, both effector and regulatory T cells contribute to IL-10 production. Therefore, T cell-derived IL-10 is an important source of IL-10 for the regulation of the Th17 response during NSV infection.

Acknowledgments

The authors thank Drs. Jay Bream, Alan Scott, Kimberly Schultz, and Victoria Baxter for their helpful discussions. This work was supported by research grants R01 NS087539 (D. E. G) and F31 NS076223 (K. A. K.) from the National Institutes of Health. The sponsor had no role in study design; in collection, analysis or interpretation of the data; in writing the report or in the decision to submit the article for publication.

References

Chaudhry, A., Samstein, R.M., Treuting, P., Liang, Y., Pils, M.C., Heinrich, J.-M., Jack, R.S., Wunderlich, F.T., Brüning, J.C., Müller, W., Rudensky, A.Y., 2011. Interleukin-10 signaling in regulatory T cells is required for suppression of Th17 cell-mediated inflammation. Immunity 34, 566–578.

Clausen, B.E., Burkhardt, C., Reith, W., Renkawitz, R., Förster, I., 1999. Conditional gene targeting in macrophages and granulocytes using LysMcre mice. Transgenic Res. 8, 265–277.

Couper, K.N., Blount, D.G., Riley, E.M., 2008. IL-10: the master regulator of immunity to infection. J. Immunol. 180, 5771–5777.

Go, Y.Y., Balasuriya, U.B.R., Lee, C.-K., 2014. Zoonotic encephalitides caused by arboviruses: transmission and epidemiology of alphaviruses and flaviviruses. Clin Exp Vaccine Res 3, 58–77.

Goldmann, T., Wieghofer, P., Müller, P.F., Wolf, Y., Varol, D., Yona, S., Brendecke, S.M., Kierdorf, K., Staszewski, O., Datta, M., Luedde, T., Heikenwalder, M., Jung, S., Prinz, M., 2013. A new type of microglia gene targeting shows TAK1 to be pivotal in CNS autoimmune inflammation. Nat. Neurosci. 16, 1618–1626.

Greene, I.P., Lee, E.-Y., Prow, N., Ngwang, B., Griffin, D.E., 2008. Protection from fatal viral encephalomyelitis: AMPA receptor antagonists have a direct effect on the inflammatory response to infection. Proc. Natl. Acad. Sci. U. S. A. 105, 3575–3580.

Hollidge, B.S., González-Scarano, F., Soldan, S.S., 2010. Arboviral encephalitides: transmission, emergence, and pathogenesis. J. NeuroImmune Pharmacol. 5, 428–442.

Huber, S., Gagliani, N., Esplugues, E., O'Connor Jr., W., Huber, F.J., Chaudhry, A., Kamanaka, M., Kobayashi, Y., Booth, C.J., Rudensky, A.Y., Roncarolo, M.G., Battaglia, M., Flavell, R.A., 2011. Th17 cells express interleukin-10 receptor and are controlled by Foxp3- and Foxp3+ regulatory CD4+ T cells in an interleukin-10-dependent manner. Immunity 34, 554–565.

Jackson, A.C., Moench, T.R., Trapp, B.D., Griffin, D.E., 1988. Basis of neurovirulence in Sindbis virus encephalomyelitis of mice. Lab. Investig. 58, 503–509.

Johnson, R.T., 1965. Virus invasion of the central nervous system: a study of Sindbis virus infection in the mouse using fluorescent antibody. Am. J. Pathol. 46, 929–943.

Kuhn, R., Lohler, J., Rennick, D., Rajewsky, K., Muller, W., 1993. Interleukin-10-deficient mice develop chronic enterocolitis. Cell 75, 263–274.

Kulcsar, K.A., Baxter, V.K., Greene, I.P., Griffin, D.E., 2014. Interleukin 10 modulation of pathogenic Th17 cells during fatal alphavirus encephalomyelitis. Proc. Natl. Acad. Sci. U. S. A. 111, 16053–16058.

Kulcsar, K.A., Baxter, V.K., Abraham, R., Nelson, A., Griffin, D.E., 2015. Distinct immune responses in resistant and susceptible strains of mice during neurovirulent alphavirus encephalomyelitis. J. Virol. 89, 8280–8291.

Lee, E.-Y., Schultz, K.L.W., Griffin, D.E., 2013. Mice deficient in interferon-gamma or interferon-gamma receptor 1 have distinct inflammatory responses to acute viral encephalomyelitis. PLoS One 8, e76412.

Li, M.O., Flavell, R.A., 2008. Contextual regulation of inflammation: a duet by transforming growth factor-β and interleukin-10. Immunity 28, 468–476.

Lin, M.T., Hinton, D.R., Parra, B., Stohlman, S.A., van der Veen, R.C., 1998. The role of IL-10 in mouse hepatitis virus-induced demyelinating encephalomyelitis. Virology 245, 270–280.

Madan, R., Demircik, F., Surianarayanan, S., Allen, J.L., Divanovic, S., Trompette, A., Yogev, N., Gu, Y., Khodoun, M., Hildeman, D., Boespflug, N., Fogolin, M.B., Grobe, L., Greweling, M., Finkelman, F.D., Cardin, R., Mohrs, M., Müller, W., Waisman, A., Roers, A., Karp, C.L., 2009. Nonredundant roles for B cell-derived IL-10 in immune counter-regulation. J. Immunol. 183, 2312–2320.

McKinstry, K.K., Strutt, T.M., Buck, A., Curtis, J.D., Dibble, J.P., Huston, G., Tighe, M., Hamada, H., Sell, S., Dutton, R.W., Swain, S.L., 2009. IL-10 deficiency unleashes an influenza-specific Th17 response and enhances survival against high-dose challenge. J. Immunol. 182, 7353–7363.

Moore, K.W., de Waal Malefyt, R., Coffman, R.L., O'Garra, A., 2001. Interleukin-10 and the interleukin-10 receptor. Annu. Rev. Immunol. 19, 683–765.

Palmer, E.M., Holbrook, B.C., Arimilli, S., Parks, G.D., Alexander-Miller, M.A., 2010. IFNγ-producing, virus-specific CD8+ effector cells acquire the ability to produce IL-10 as a result of entry into the infected lung environment. Virology 404, 225–230.

Puntambekar, S.S., Bergmann, C.C., Savarin, C., Karp, C.L., Phares, T.W., Parra, G.I., Hinton, D.R., Stohlman, S.A., 2011. Shifting hierarchies of interleukin-10-producing T cell populations in the central nervous system during acute and persistent viral encephalomyelitis. J. Virol. 85, 6702–6713.

Roers, A., Siewe, L., Strittmatter, E., Deckert, M., Schlüter, D., Stenzel, W., Gruber, A.D., Krieg, T., Rajewsky, K., Müller, W., 2004. T cell-specific inactivation of the interleukin 10 gene in mice results in enhanced T cell responses but normal innate responses to lipopolysaccharide or skin irritation. J Exp Med 200, 1289–1297.

Rowell, J.F., Griffin, D.E., 2002. Contribution of T cells to mortality in neurovirulent Sindbis virus encephalomyelitis. J. Neuroimmunol. 127, 106–114.

Saraiva, M., O'Garra, A., 2010. The regulation of IL-10 production by immune cells. Nat Rev Immunol 10, 170–181.

Siewe, L., Bollati Fogolin, M., Wickenhauser, C., Krieg, T., Müller, W., Roers, A., 2006. Interleukin-10 derived from macrophages and/or neutrophils regulates the inflammatory response to LPS but not the response to CpG DNA. Eur. J. Immunol. 36, 3248–3255.

Sun, J., Madan, R., Karp, C.L., Braciale, T.J., 2009. Effector T cells control lung inflammation during acute influenza virus infection by producing IL-10. Nat. Med. 15, 277–284.

Taylor, R.M., Hurlbut, H.S., Work, T.H., Kingston, J.R., Frothingham, T.E., 1955. Sindbis virus: a newly recognized arthropodtransmitted virus. Am.J.Trop. Med. Hyg. 4, 844–862.

Thach, D.C., Kimura, T., Griffin, D.E., 2000. Differences between C57BL/6 and BALB/cBy mice in mortality and virus replication after intranasal infection with neuroadapted Sindbis virus. J. Virol. 74, 6156–6161.

Trandem, K., Anghelina, D., Zhao, J., Perlman, S., 2010. Regulatory T cells inhibit T cell proliferation and decrease demyelination in mice chronically infected with a coronavirus. J. Immunol. 184, 4391–4400.

Trandem, K., Jin, Q., Weiss, K.A., James, B.R., Zhao, J., Perlman, S., 2011a. Virally expressed interleukin-10 ameliorates acute encephalomyelitis and chronic demyelination in coronavirus-infected mice. J. Virol. 85, 6822–6831.

Trandem, K., Zhao, J., Fleming, E., Perlman, S., 2011b. Highly activated cytotoxic CD8 T cells express protective IL-10 at the peak of coronavirus-induced encephalitis. J. Immunol. 186, 3642–3652.

Wack, A., Openshaw, P., O'Garra, A., 2011. Contribution of cytokines to pathology and protection in virus infection. Curr Opin Virol 1, 184–195.

Zhao, J., Zhao, J., Perlman, S., 2014. Virus-specific regulatory T cells ameliorate encephalitis by repressing effector T cell functions from priming to effector stages. PLoS Pathog. 10, e1004279.